U-Th-Pb discordia regression

Pieter Vermeesch

London Geochronology Centre, Department of Earth Sciences, University College London, United Kingdom

Correspondence: Pieter Vermeesch (p.vermeesch@ucl.ac.uk)

Abstract. The actinide elements U and Th undergo radioactive decay to three isotopes of Pb, forming the basis of three coupled geochronometers. The ^{206}Pb/^{238}U and ^{207}Pb/^{235}U decay systems are routinely combined to improve accuracy. Joint consideration with the ^{208}Pb/^{232}Th decay system is less common. This paper aims to change this. Co-measured ^{208}Pb/^{232}Th is particularly useful for discordant samples containing variable amounts of non-radiogenic ('common') Pb.

5   The paper presents a maximum likelihood algorithm for joint isochron regression of the ^{206}Pb/^{238}Pb, ^{207}Pb/^{235}Pb, and ^{208}Pb/^{232}Th chronometers. Given a set of cogenetic samples, the algorithm estimates the common Pb composition and concordia intercept age. U-Th-Pb data can be visualised on a conventional Wetherill or Tera-Wasserburg concordia diagram, or on a ^{208}Pb/^{232}Th vs. ^{206}Pb/^{238}U plot. Alternatively, the results of the new discordia regression algorithm can also be visualised as a ^{208}Pb$_c$/^{206}Pb vs. ^{238}U/^{206}Pb or ^{208}Pb$_c$/^{207}Pb vs. ^{238}U/^{207}Pb isochron, where ^{208}Pb$_c$ represents the common ^{208}Pb component.

10   For detrital minerals, it is generally not safe to assume a shared common Pb composition and concordia intercept age. In this case the U-Th-Pb discordia regression method must be modified by tying it to a terrestrial lead evolution model. Thus also detrital common Pb correction can be formulated in a maximum likelihood sense.

The new method was applied to a published monazite dataset with a Th/U-ratio of ~ 10, resulting in a significant radiogenic ^{208}Pb component. Therefore the case study represents a 'worst case scenario' for the new algorithm. Nevertheless, it manages

15   to fit the data very well. The method should work even better in low-Th phases such as carbonates. The degree to which the dispersion of the data around the isochron line matches the analytical uncertainties can be assessed using the mean square of the weighted deviates (MSWD) statistic. A modified four parameter version of the regression algorithm quantifies this overdispersion, providing potentially valuable geological insight into the processes that control isotopic closure.

All the parameters in the discordia regression method (including the age and the overdispersion parameter) are strictly

20   positive quantities that exhibit skewed error distributions near zero. This skewness can be accounted for using the profile log-likelihood method, or by recasting the regression algorithm in terms of logarithmic quantities. Both approaches yield realistic asymmetric confidence intervals for the model parameters. The new algorithm is flexible enough that it can accommodate disequilibrium corrections and inter-sample error correlations when these are provided by the user. All the methods presented in this paper have been added to the `IsoplotR` software package. This will hopefully encourage geochronologists to take full

25   advantage of the entire U-Th-Pb decay system.

1 Introduction

The lead content of uranium-bearing minerals comprises two components:

1. Non-radiogenic (a.k.a. initial or 'common') Pb is inherited from the environment during crystallisation. It contains all of lead's four stable isotopes (^{204}Pb, ^{206}Pb, ^{207}Pb and ^{208}Pb) in fixed proportions for a given sample.

30 2. Radiogenic Pb is added to the common Pb after crystallisation due to the decay of U and Th. It contains only three isotopes (^{206}Pb, ^{207}Pb and ^{208}Pb), which occur in variable proportions as a function of the Th/U-ratio and age.

Denoting the measured and non-radiogenic components with subscripts 'm' and 'c' respectively, and assuming initial secular equilibrium, we can write:

$$^{204}Pb_m = {}^{204}Pb_c \tag{1}$$

35 $$^{206}Pb_m = {}^{206}Pb_c + {}^{238}U_m \left(e^{\lambda_{38}t} - 1\right) \tag{2}$$

$$^{207}Pb_m = {}^{207}Pb_c + {}^{235}U_m \left(e^{\lambda_{35}t} - 1\right) \tag{3}$$

$$^{208}Pb_m = {}^{208}Pb_c + {}^{232}Th_m \left(e^{\lambda_{32}t} - 1\right) \tag{4}$$

where λ_{38}, λ_{35} and λ_{32} are the decay constants of ^{238}U, ^{235}U and ^{232}Th, respectively, and t is the time elapsed since isotopic closure. In order to accurately estimate t, the common Pb composition is needed. One way to account for common Pb is to

40 normalise all the measurements to ^{204}Pb. For example, using the ^{238}U – ^{206}Pb decay scheme:

$$\left[\frac{^{206}Pb}{^{204}Pb}\right]_m = \left[\frac{^{206}Pb}{^{204}Pb}\right]_c + \left[\frac{^{238}U}{^{204}Pb}\right]_m \left(e^{\lambda_{38}t} - 1\right) \tag{5}$$

Applying Equation 5 to multiple cogenetic aliquots of the same sample defines an isochron with slope $\left(e^{\lambda_{38}t} - 1\right)$ and intercept $\left[^{206}Pb/^{204}Pb\right]_c$. Alternatively, and equivalently, an 'inverse' isochron line can be defined as:

$$\left[\frac{^{204}Pb}{^{206}Pb}\right]_m = \left[\frac{^{204}Pb}{^{206}Pb}\right]_c \left\{1 - \left[\frac{^{238}U}{^{206}Pb}\right]_m \left(e^{\lambda_{38}t} - 1\right)\right\} \tag{6}$$

45 In this case, the isochron is a line whose y-intercept defines the common ^{204}Pb/^{206}Pb-ratio, and the x-intercept determines the radiogenic ^{238}U/^{206}Pb-ratio.

  The isochron concept can easily be applied to the ^{235}U – ^{207}Pb system, by replacing ^{206}Pb with ^{207}Pb, ^{238}Pb with ^{235}Pb and λ_{38} with λ_{35} in Equations 5 and 6. The accuracy and precision of the calculation can be further improved by solving the

50 ^{206}Pb/^{238}U and ^{207}Pb/^{235}U isochron equations simultaneously and requiring t to be the same in both systems. The resulting three-dimensional constrained isochron is known as a 'Total-Pb/U isochron' and represents the pinnacle of statistical rigour in U-Pb geochronology (Ludwig, 1998).

In igneous samples, the conventional total Pb/U isochron requires isotopic data for two or more cogenetic aliquots. In the simplest case, a two-point isochron can be formed by analysing the U-Pb composition of the U-bearing phase of interest along with a cogenetic mineral devoid of U (e.g, feldspar). In detrital samples, the common Pb intercept of the isochron can be anchored to some nominal value, or to a terrestrial lead evolution model (e.g., Stacey and Kramers, 1975). Thus, the [204]Pb-based total U-Pb isochron method is beneficial to nearly all applications of the U-Pb method.

Unfortunately, [204]Pb-based common Pb correction is not always practical. First, not all mass spectrometers are able to measure [204]Pb with sufficient precision and accuracy. In ICP-MS instruments, the presence of an isobaric interference with [204]Hg precludes accurate [204]Pb measurements. And second, because [204]Pb is by far the least abundant of lead's four naturally occurring isotopes, it requires the longest dwell times. For single collector instruments, this degrades the precision of the other isotopes to the point where the analytical cost of measuring [204]Pb may outweigh its benefits.

One way to overcome both problems is to use the [232]Th – [208]Pb decay scheme to determine the common Pb component. Thus, if we can estimate $^{208}Pb_c$ in Equation 4, then Equation 5 can be replaced with:

$$\frac{^{206}Pb_m}{^{208}Pb_c} = \left[\frac{^{206}Pb}{^{208}Pb}\right]_c + \frac{^{238}U_m}{^{208}Pb_c}\left(e^{\lambda_{38}t} - 1\right) \tag{7}$$

and similarly for Equation 6 and the [235]U – [207]Pb equivalents of Equations 5 and 6.

This paper introduces a 'U-Th-Pb isochron' algorithm that achieves this reformulation. The algorithm is similar to Ludwig (1998)'s total Pb/U isochron, but uses a unified approach that accommodates both random and systematic uncertainties. The algorithms introduced in this paper will be illustrated using a published U-Th-Pb dataset for monazite grain #10 in sample BHE-01 of Gibson et al. (2016). With a Th/U-ratio of ~ 10, this sample represents a 'worst case scenario' in the sense that the addition of lots of radiogenic [208]Pb complicates the removal of the common Pb component. The fact that the new algorithm works very well for monazite implies that it is generally applicable low Th phases such as carbonates.

2 U-Th-Pb concordia

In conventional U-Pb geochronology, the set of concordant [206]Pb/[238]U- and [207]Pb/[235]U-ratios defines a 'Wetherill' concordia line. Similarly, U-Th-Pb data can be visualised in [208]Pb/[232]Th- vs. [206]Pb/[238]U-ratio space (Figure 1.a). In the absence of common Pb, samples whose [208]Pb/[232]Th-ages equal their [206]Pb/[238]U-ages plot on a U-Th-Pb concordia line. The addition of common Pb pulls samples away from this line. Common Pb correction amounts to moving samples back to concordia:

$$\left[\frac{^{208}Pb}{^{232}Th}\right]_* = \left[\frac{^{208}Pb}{^{232}Th}\right]_m - \frac{^{208}Pb_c}{^{232}Th_m} \tag{8}$$

$$\left[\frac{^{206}Pb}{^{238}U}\right]_* = \left[\frac{^{206}Pb}{^{238}U}\right]_m - \left[\frac{^{206}Pb}{^{208}Pb}\right]_c \frac{^{208}Pb_c}{^{232}Th_m}\left[\frac{^{232}Th}{^{238}U}\right]_m \tag{9}$$
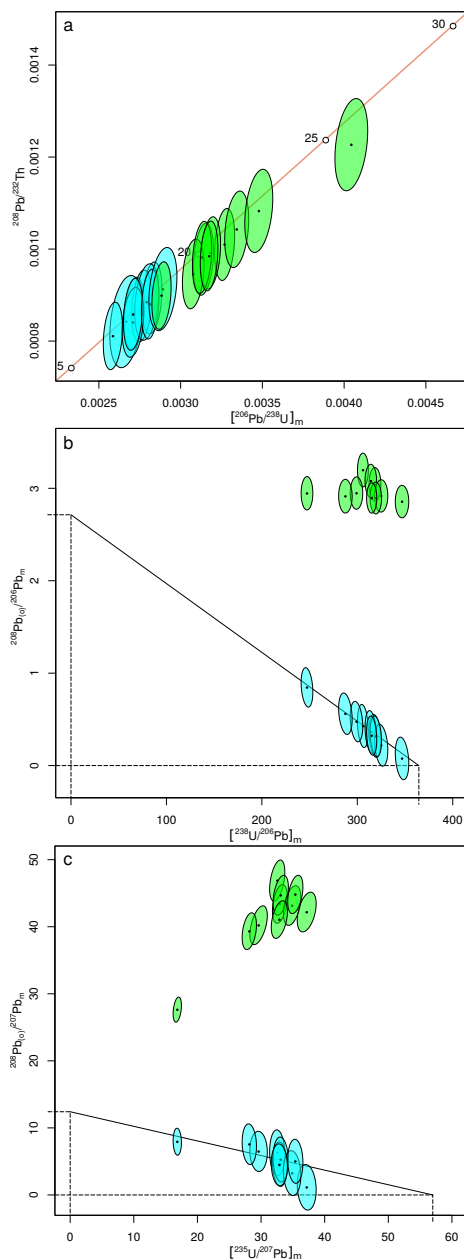
Figure 1. a. U-Th-Pb concordia diagram showing ^{206}Pb/^{238}U and ^{208}Pb/^{232}Th ratios for monazite grain #10 in sample BHE-01 of Gibson et al. (2016). Uncorrected ratios are shown in green and common Pb corrected ratios in blue. b. ^{238}U-^{232}Th-^{206,208}Pb and c. ^{235}U-^{232}Th-^{207,208}Pb isochron plots for the Gibson et al. (2016) dataset. Green ellipses represent the raw data. Blue ellipses show the same measurements with the radiogenic ^{208}Pb removed. The x-intercept of the two resulting isochrons yield the radiogenic U-Pb composition, and correspond to an age of 17.66 Ma. The y-intercepts of the yield the common Pb isotopic composition, with $\left[^{208}Pb/^{206}Pb\right]_c = 2.71$ and $\left[^{208}Pb/^{207}Pb\right]_c = 12.41$.

where '∗' marks the radiogenic component. Figure 1.a shows the effect of this correction on the Gibson et al. (2016) data, using

85 $\left[{}^{206}Pb/{}^{208}Pb\right]_c = 0.3685$ and a variable ${}^{208}Pb_c/{}^{232}Th_m$-ratio calculated by rearranging Equation 4 for $t = 17.66$ Ma.

An alternative visualisation is to plot the ^{208}Pb/^{206}Pb against ^{238}U/^{206}Pb (green ellipses in Figure 1.b,c). Removing the radiogenic ^{208}Pb-component and plotting ^{208}Pb$_c$/^{206}Pb against ^{238}U/^{206}Pb creates a linear isochron array (blue ellipses in Figure 1.b). The x-intercept of this line equals the radiogenic U-Pb composition whilst the y-intercept equals its common Pb composition.

90 The same exercise can be repeated for ^{208}Pb/^{207}Pb and ^{235}U/^{207}Pb (Figure 1.c). The linear fit corresponds to a concordant U-Pb age of 17.66 Ma and a common Pb composition with $\left[{}^{208}Pb/{}^{206}Pb\right]_c = 2.56$ and $\left[{}^{208}Pb/{}^{207}Pb\right]_c = 11.71$. The next section of this paper introduces an algorithm to automatically find this optimal solution and propagate the corresponding uncertainties.

3 The U-Th-Pb isochron

The U-Th-Pb isochron line is constrained by three free parameters, the age (t) and the common Pb composition (α, β) where:

95 $$\alpha = \left[\frac{{}^{206}Pb}{{}^{208}Pb}\right]_c \text{ and } \beta = \left[\frac{{}^{207}Pb}{{}^{208}Pb}\right]_c \tag{10}$$

t, α and β can be estimated by minimising the sum of squares:

$$S = \Delta^T \Sigma_\Delta^{-1} \Delta = \begin{bmatrix} K^T & L^T & M^T \end{bmatrix} \begin{bmatrix} \Omega_{1,1} & \Omega_{1,2} & \Omega_{1,3} \\ \Omega_{2,1} & \Omega_{2,2} & \Omega_{2,3} \\ \Omega_{3,1} & \Omega_{3,2} & \Omega_{3,3} \end{bmatrix} \begin{bmatrix} K \\ L \\ M \end{bmatrix} \tag{11}$$

with

$$K = X - U\beta W\gamma - e^{\lambda_{35}t} + 1 \tag{12}$$
100 $$L = Y - \alpha W\gamma - e^{\lambda_{38}t} + 1 \tag{13}$$
$$M = Z - \gamma - e^{\lambda_{32}t} + 1 \tag{14}$$

where U is the ^{238}U/^{235}U-ratio (= 137.818; Hiess et al., 2012),

$$X = \left[\frac{{}^{207}Pb}{{}^{235}U}\right]_m, Y = \left[\frac{{}^{206}Pb}{{}^{238}U}\right]_m \text{ and } Z = \left[\frac{{}^{208}Pb}{{}^{232}Th}\right]_m \tag{15}$$

are n-element column vectors containing the ^{207}Pb/^{235}U-, ^{206}Pb/^{238}U-, and ^{208}Pb/^{232}Th-measurements,

105 $$W = \left[\frac{{}^{232}Th}{{}^{238}U}\right]_m \tag{16}$$

is an $n \times n$ diagonal matrix with the ^{232}Th/^{238}U-measurements, and

$$\gamma = \frac{{}^{208}Pb_c}{{}^{232}Th_m} \tag{17}$$

is an n-element column vector with the inherited ^{208}Pb/^{232}Th-ratios. γ is unknown but can be estimated from the data along with the scalars t, α, and β.

110

Σ_Δ is the covariance matrix of the misfit parameters K, L and M. This matrix is obtained by error propagation of the isotopic measurement and decay constant uncertainties:

$$\Sigma_\Delta = J^T \Sigma J \tag{18}$$

where

$$\Sigma = \begin{bmatrix} s[X]^2 & s[X,Y] & s[X,Z] & 0_{n\times1} & 0_{n\times1} & 0_{n\times1} \\ s[Y,X] & s[Y]^2 & s[Y,Z] & 0_{n\times1} & 0_{n\times1} & 0_{n\times1} \\ s[Z,X] & s[Z,Y] & s[Z]^2 & 0_{n\times1} & 0_{n\times1} & 0_{n\times1} \\ 0_{1\times n} & 0_{1\times n} & 0_{1\times n} & s[\lambda_{35}]^2 & 0 & 0 \\ 0_{1\times n} & 0_{1\times n} & 0_{1\times n} & 0 & s[\lambda_{38}]^2 & 0 \\ 0_{1\times n} & 0_{1\times n} & 0_{1\times n} & 0 & 0 & s[\lambda_{32}]^2 \end{bmatrix} \tag{19}$$

115

in which

$$s[X]^2 = I_{n\times n} \begin{bmatrix} s[X_1]^2 \\ \vdots \\ s[X_i] \\ \vdots \\ s[X_n]^2 \end{bmatrix}, \; s[X,Y] = I_{n\times n} \begin{bmatrix} s[X_1,Y_1] \\ \vdots \\ s[X_i,Y_i] \\ \vdots \\ s[X_n,Y_n] \end{bmatrix}$$

and so forth, where $I_{n\times n}$ marks the $n \times n$ identity matrix, and $s[X_i]^2$ and $s[X_i,Y_i]$ represent the variance and covariance of X_i and Y_i, respectively. The Jacobian matrix J is given by:

$$J = \begin{bmatrix} 1_{n,n} & 0_{n\times n} & 0_{n\times n} \\ 0_{n\times n} & 1_{n\times n} & 0_{n\times n} \\ 0_{n\times n} & 0_{n\times n} & 1_{n\times n} \\ -t_{1\times n}e^{\lambda_{35}t} & 0_{1\times n} & 0_{1\times n} \\ 0_{1\times n} & -t_{1\times n}e^{\lambda_{38}t} & 0_{1\times n} \\ 0_{1\times n} & 0_{1\times n} & -t_{1\times n}e^{\lambda_{32}t} \end{bmatrix} \tag{20}$$

120

where $1_{a\times b}$, $0_{a\times b}$ and $t_{a\times b}$ are $a \times b$ matrices filled with 1s, 0s and ts, respectively.

To minimise S with respect to t, α and β, we first need to estimate γ for any given value of these free parameters. To this end, we replace γ by $Z - M - e^{\lambda_{32}t} + 1$ in Equation 14, so that:

125 $\quad K = \hat{K} + U\beta WM$ with $\hat{K} = X - U\beta W(Z - e^{\lambda_{32}t} + 1) - e^{\lambda_{35}t} + 1 \tag{21}$

and

$$L = \hat{L} + \alpha W M \text{ with } \hat{L} = Y - \alpha W(Z - e^{\lambda_{32} t} + 1) - e^{\lambda_{38} t} + 1 \tag{22}$$

Plugging Equations 21 and 22 into Equation 11 and rearranging yields:

$$S = M^T A M + B M + M^T C + D \tag{23}$$

where

$$A = U^2 \beta^2 W_d \Omega_{1,1} W_d + \alpha^2 W_d \Omega_{2,2} W_d + \Omega_{3,3} + U \alpha \beta W_d (\Omega_{1,2} + \Omega_{2,1}) W_d +$$
$$U \beta (W_d \Omega_{1,3} + \Omega_{3,1} W_d) + \alpha (W_d \Omega_{2,3} + \Omega_{3,2} W_d) \tag{24}$$

$$B = U \beta \hat{K}^T \Omega_{1,1} W_d + \alpha \hat{L}^T \Omega_{2,2} W_d + \alpha \hat{K}^T \Omega_{1,2} W_d + U \beta \hat{L}^T \Omega_{2,1} W_d + \hat{K}^T \Omega_{1,3} + \hat{L}^T \Omega_{2,3} \tag{25}$$

$$C = U \beta W_d \Omega_{1,1} \hat{K} + \alpha W_d \Omega_{2,2} \hat{L} + U \beta W_d \Omega_{1,2} \hat{L} + \alpha W_d \Omega_{2,1} \hat{K} + \Omega_{3,1} \hat{K} + \Omega_{3,2} \hat{L} \tag{26}$$

$$D = \hat{K}^T \Omega_{1,1} \hat{K} + \hat{K}^T \Omega_{1,2} \hat{L} + \hat{L}^T \Omega_{2,1} \hat{K} + \hat{L}^T \Omega_{2,2} \hat{L} \tag{27}$$

Taking the matrix derivative of S with respect to M:

$$\partial S / \partial M = M^T (A + A^T) + B + C^T \tag{28}$$

Setting $\partial S / \partial M = 0$ and solving for M:

$$M = -(A + A^T)^{-1}(B^T + C) \tag{29}$$

Plugging M back into Equation 14 yields our estimate of γ, which allows us to calculate S. The values of t, α and β that minimise S are then found by numerical methods.

4 Error propagation

The log-likelihood of the isochron fit is given by

$$\mathcal{L} = -\frac{1}{2} \left[3 \ln(2\pi) + \ln |\Sigma_\Delta| + S \right] \tag{30}$$

where $|\Sigma_\Delta|$ is the determinant of Σ_Δ. The covariance matrix of the three fit parameters is then obtained by inverting the matrix of second derivates of the negative log-likelihood with respect to the vector γ and the scalars t, α, β (the Fisher Information matrix):

150

$$
\begin{bmatrix}
\Sigma\gamma & s[\gamma,t] & s[\gamma,\alpha] & s[\gamma,\beta] \\
s[t,\gamma] & s[t]^2 & s[t,\alpha] & s[t,\beta] \\
s[\alpha,\gamma] & s[\alpha,t] & s[\alpha]^2 & s[\alpha,\beta] \\
s[\beta,\gamma] & s[\beta,t] & s[\beta,\alpha] & s[\beta]^2
\end{bmatrix}
= -
\begin{bmatrix}
\frac{\partial^2 \mathcal{L}}{\partial \gamma^2} & \frac{\partial^2 \mathcal{L}}{\partial \gamma \partial t} & \frac{\partial^2 \mathcal{L}}{\partial \gamma \partial \alpha} & \frac{\partial^2 \mathcal{L}}{\partial \gamma \partial \beta} \\
\frac{\partial^2 \mathcal{L}}{\partial t \partial \gamma} & \frac{\partial^2 \mathcal{L}}{\partial t^2} & \frac{\partial^2 \mathcal{L}}{\partial t \partial \alpha} & \frac{\partial^2 \mathcal{L}}{\partial t \partial \beta} \\
\frac{\partial^2 \mathcal{L}}{\partial \alpha \partial \gamma} & \frac{\partial^2 \mathcal{L}}{\partial \alpha \partial t} & \frac{\partial^2 \mathcal{L}}{\partial \alpha^2} & \frac{\partial^2 \mathcal{L}}{\partial \alpha \partial \beta} \\
\frac{\partial^2 \mathcal{L}}{\partial \beta \partial \gamma} & \frac{\partial^2 \mathcal{L}}{\partial \beta \partial t} & \frac{\partial^2 \mathcal{L}}{\partial \beta \partial \alpha} & \frac{\partial^2 \mathcal{L}}{\partial \beta^2}
\end{bmatrix}^{-1}
\tag{31}
$$

where Σ_γ is an $n \times n$ matrix; $s[\gamma,t]$, $s[\gamma,\alpha]$ and $s[\gamma,\beta]$ are n-element row vectors, $s[t,\gamma]$, $s[\alpha,\gamma]$ and $s[\beta,\gamma]$ are n-element column vectors, and all other elements are scalars. The second derivatives are as follows:

$$
\frac{\partial^2 \mathcal{L}}{\partial \gamma^2} = -
\begin{bmatrix} U\beta W \\ \alpha W \\ I_{n \times n} \end{bmatrix}^T
\Sigma_\Delta^{-1}
\begin{bmatrix} U\beta W \\ \alpha W \\ I_{n \times n} \end{bmatrix}
\tag{32}
$$

155

$$
\frac{\partial^2 \mathcal{L}}{\partial \gamma \partial t} = \left(\frac{\partial^2 \mathcal{L}}{\partial t \partial \gamma} \right)^T = -
\begin{bmatrix} U\beta W \\ \alpha W \\ I_{n \times n} \end{bmatrix}^T
\Sigma_\Delta^{-1}
\begin{bmatrix} (\lambda_{35} e^{\lambda_{35} t})_{n \times 1} \\ (\lambda_{38} e^{\lambda_{38} t})_{n \times 1} \\ (\lambda_{32} e^{\lambda_{32} t})_{n \times 1} \end{bmatrix}
\tag{33}
$$

$$
\frac{\partial^2 \mathcal{L}}{\partial \gamma \partial \alpha} = \left(\frac{\partial^2 \mathcal{L}}{\partial \alpha \partial \gamma} \right)^T =
\begin{bmatrix} 0_{n \times n} \\ W \\ 0_{n \times n} \end{bmatrix}^T
\Sigma_\Delta^{-1} \Delta -
\begin{bmatrix} U\beta W \\ \alpha W \\ I_{n \times n} \end{bmatrix}^T
\Sigma_\Delta^{-1}
\begin{bmatrix} 0_{n \times 1} \\ W\gamma \\ 0_{n \times 1} \end{bmatrix}
\tag{34}
$$

$$
\frac{\partial^2 \mathcal{L}}{\partial \gamma \partial \beta} = \left(\frac{\partial^2 \mathcal{L}}{\partial \beta \partial \gamma} \right)^T =
\begin{bmatrix} UW \\ 0_{n \times n} \\ 0_{n \times n} \end{bmatrix}^T
\Sigma_\Delta^{-1} \Delta -
\begin{bmatrix} U\beta W \\ \alpha W \\ I_{n \times n} \end{bmatrix}^T
\Sigma_\Delta^{-1}
\begin{bmatrix} UW\gamma \\ 0_{n \times 1} \\ 0_{n \times 1} \end{bmatrix}
\tag{35}
$$

160

$$
\frac{\partial^2 \mathcal{L}}{\partial t^2} = \Delta^T \Sigma_\Delta^{-1}
\begin{bmatrix} (e^{\lambda_{35} t} \lambda_{35}^2)_{n \times 1} \\ (e^{\lambda_{38} t} \lambda_{38}^2)_{n \times 1} \\ (e^{\lambda_{32} t} \lambda_{32}^2)_{n \times 1} \end{bmatrix} -
\begin{bmatrix} (\lambda_{35} e^{\lambda_{35} t})_{n \times 1} \\ (\lambda_{38} e^{\lambda_{38} t})_{n \times 1} \\ (\lambda_{32} e^{\lambda_{32} t})_{n \times 1} \end{bmatrix}^T
\Sigma_\Delta^{-1}
\begin{bmatrix} (\lambda_{35} e^{\lambda_{35} t})_{n \times 1} \\ (\lambda_{38} e^{\lambda_{38} t})_{n \times 1} \\ (\lambda_{32} e^{\lambda_{32} t})_{n \times 1} \end{bmatrix}
\tag{36}
$$

$$
\frac{\partial^2 \mathcal{L}}{\partial t \partial \alpha} = \frac{\partial^2 \mathcal{L}}{\partial \alpha \partial t} = -
\begin{bmatrix} 0_{1 \times n} \\ W\gamma \\ 0_{1 \times n} \end{bmatrix}^T
\Sigma_\Delta^{-1}
\begin{bmatrix} (\lambda_{35} e^{\lambda_{35} t})_{n \times 1} \\ (\lambda_{38} e^{\lambda_{38} t})_{n \times 1} \\ (\lambda_{32} e^{\lambda_{32} t})_{n \times 1} \end{bmatrix}
\tag{37}
$$

165
$$\frac{\partial^2 \mathcal{L}}{\partial t \partial \beta} = \frac{\partial^2 \mathcal{L}}{\partial \beta \partial t} = - \begin{bmatrix} UW\gamma \\ 0_{n\times1} \\ 0_{n\times1} \end{bmatrix}^T \Sigma_\Delta^{-1} \begin{bmatrix} (\lambda_{35} e^{\lambda_{35} t})_{n\times1} \\ (\lambda_{38} e^{\lambda_{38} t})_{n\times1} \\ (\lambda_{32} e^{\lambda_{32} t})_{n\times1} \end{bmatrix} \tag{38}$$

$$\frac{\partial^2 \mathcal{L}}{\partial \alpha^2} = - \begin{bmatrix} 0_{n\times1} \\ W\gamma \\ 0_{n\times1} \end{bmatrix}^T \Sigma_\Delta^{-1} \begin{bmatrix} 0_{n\times1} \\ W\gamma \\ 0_{n\times1} \end{bmatrix} \tag{39}$$

$$\frac{\partial^2 \mathcal{L}}{\partial \beta^2} = - \begin{bmatrix} UW\gamma \\ 0_{n\times1} \\ 0_{n\times1} \end{bmatrix}^T \Sigma_\Delta^{-1} \begin{bmatrix} UW\gamma \\ 0_{n\times1} \\ 0_{n\times1} \end{bmatrix} \tag{40}$$

170

$$\frac{\partial^2 \mathcal{L}}{\partial \alpha \partial \beta} = \frac{\partial^2 \mathcal{L}}{\partial \beta \partial \alpha} = - \begin{bmatrix} UW\gamma \\ 0_{n\times1} \\ 0_{n\times1} \end{bmatrix}^T \Sigma_\Delta^{-1} \begin{bmatrix} 0_{n\times1} \\ W\gamma \\ 0_{n\times1} \end{bmatrix} \tag{41}$$

The Fisher Information matrix is best solved by block matrix inversion. This is achieved by partitioning Equation 31 into four parts, with $\partial^2 \mathcal{L}/\partial \gamma^2$ defining the first block.

5 Overdispersion

175 If analytical uncertainty is the only source of data scatter around the discordia line, then the sum of squares S follows a central Chi-square distribution with $2n-3$ degrees of freedom (i.e., χ^2_{2n-3}). Normalising S by the degrees of freedom gives rise to the so-called reduced Chi-square statistic, which is also known as the Mean Square of the Weighted Deviates (MSWD):

$$MSWD = \frac{S}{2n-3} \tag{42}$$

Datasets are said to be *overdispersed* if S is greater than the 95% percentile of χ^2_{2n-3} or, equivalently, if $MSWD \gg 1$. This
180 is the case for the Gibson et al. (2016) dataset, whose MSWD = 8.6 (p-value ≈ 0). The overdispersion can be attributed to geological scatter in the concordia intercept age t. Suppose that this scatter follows a normal distribution with zero mean and let ω be the standard deviation of this distribution. Then we can redefine Σ_Δ as:

$$\Sigma_\Delta = J\Sigma J^T + J_\omega \omega^2 J_\omega^T \tag{43}$$

where

185
$$J_\omega = \begin{bmatrix} -\lambda_{35} e^{\lambda_{35} t} 1_{n\times1} \\ -\lambda_{38} e^{\lambda_{38} t} 1_{n\times1} \\ -\lambda_{32} e^{\lambda_{32} t} 1_{n\times1} \end{bmatrix} \tag{44}$$

ω can then be found by plugging Equation 43 into Equation 30 and maximising $\mathcal{L}$. Like before, the uncertainty of ω is obtained by inverting the Fisher Information, replacing Equation 31 with

$$
\begin{bmatrix}
\Sigma\gamma & s[\gamma,t] & s[\gamma,\alpha] & s[\gamma,\beta] & s[\gamma,\omega] \\
s[t,\gamma] & s[t]^2 & s[t,\alpha] & s[t,\beta] & s[t,\omega] \\
s[\alpha,\gamma] & s[\alpha,t] & s[\alpha]^2 & s[\alpha,\beta] & s[\alpha,\omega] \\
s[\beta,\gamma] & s[\beta,t] & s[\beta,\alpha] & s[\beta]^2 & s[\beta,\omega] \\
s[\omega,\gamma] & s[\omega,t] & s[\omega,\alpha] & s[\omega,\beta]^2 & s[\omega]^2
\end{bmatrix}
= -
\begin{bmatrix}
\frac{\partial^2 \mathcal{L}}{\partial\gamma^2} & \frac{\partial^2 \mathcal{L}}{\partial\gamma\partial t} & \frac{\partial^2 \mathcal{L}}{\partial\gamma\partial\alpha} & \frac{\partial^2 \mathcal{L}}{\partial\gamma\partial\beta} & \frac{\partial^2 \mathcal{L}}{\partial\gamma\partial\omega} \\
\frac{\partial^2 \mathcal{L}}{\partial t\partial\gamma} & \frac{\partial^2 \mathcal{L}}{\partial t^2} & \frac{\partial^2 \mathcal{L}}{\partial t\partial\alpha} & \frac{\partial^2 \mathcal{L}}{\partial t\partial\beta} & \frac{\partial^2 \mathcal{L}}{\partial t\partial\omega} \\
\frac{\partial^2 \mathcal{L}}{\partial\alpha\partial\gamma} & \frac{\partial^2 \mathcal{L}}{\partial\alpha\partial t} & \frac{\partial^2 \mathcal{L}}{\partial\alpha^2} & \frac{\partial^2 \mathcal{L}}{\partial\alpha\partial\beta} & \frac{\partial^2 \mathcal{L}}{\partial\alpha\partial\omega} \\
\frac{\partial^2 \mathcal{L}}{\partial\beta\partial\gamma} & \frac{\partial^2 \mathcal{L}}{\partial\beta\partial t} & \frac{\partial^2 \mathcal{L}}{\partial\beta\partial\alpha} & \frac{\partial^2 \mathcal{L}}{\partial\beta^2} & \frac{\partial^2 \mathcal{L}}{\partial\beta\partial\omega} \\
\frac{\partial^2 \mathcal{L}}{\partial\omega\partial\gamma} & \frac{\partial^2 \mathcal{L}}{\partial\omega\partial t} & \frac{\partial^2 \mathcal{L}}{\partial\omega\partial\alpha} & \frac{\partial^2 \mathcal{L}}{\partial\omega\partial\beta^2} & \frac{\partial^2 \mathcal{L}}{\partial\omega^2}
\end{bmatrix}^{-1}
\tag{45}
$$

where

$$
\frac{\partial^2 \mathcal{L}}{\partial\gamma\partial\omega} = \left(\frac{\partial^2 \mathcal{L}}{\partial\omega\partial\gamma}\right)^T = -\Delta^T \frac{\partial\Sigma_\Delta^{-1}}{\partial\omega}
\begin{bmatrix}
U\beta W \\
\alpha W \\
I_{n\times n}
\end{bmatrix}
\tag{46}
$$

$$
\frac{\partial^2 \mathcal{L}}{\partial t\partial\omega} = \left(\frac{\partial^2 \mathcal{L}}{\partial\omega\partial t}\right)^T = -\Delta^T \frac{\partial\Sigma_\Delta^{-1}}{\partial\omega}
\begin{bmatrix}
(\lambda_{35}e^{\lambda_{35}t})_{n\times 1} \\
(\lambda_{38}e^{\lambda_{38}t})_{n\times 1} \\
(\lambda_{32}e^{\lambda_{32}t})_{n\times 1}
\end{bmatrix}
\tag{47}
$$

$$
\frac{\partial^2 \mathcal{L}}{\partial\alpha\partial\omega} = \left(\frac{\partial^2 \mathcal{L}}{\partial\omega\partial\alpha}\right)^T = -\Delta^T \frac{\partial\Sigma_\Delta^{-1}}{\partial\omega}
\begin{bmatrix}
0_{n\times 1} \\
W\gamma \\
0_{n\times 1}
\end{bmatrix}
\tag{48}
$$

$$
\frac{\partial^2 \mathcal{L}}{\partial\beta\partial\omega} = \left(\frac{\partial^2 \mathcal{L}}{\partial\omega\partial\beta}\right)^T = -\Delta^T \frac{\partial\Sigma_\Delta^{-1}}{\partial\omega}
\begin{bmatrix}
UW\gamma \\
0_{n\times 1} \\
0_{n\times 1}
\end{bmatrix}
\tag{49}
$$

$$
\frac{\partial^2 \mathcal{L}}{\partial\omega^2} = -\frac{1}{2}\left(\frac{\partial^2 \ln|\Sigma_\Delta|}{\partial\omega^2} + \Delta^T \frac{\partial^2 \Sigma_\Delta^{-1}}{\partial\omega^2}\Delta\right)
\tag{50}
$$

with

$$
\frac{\partial\Sigma_\Delta^{-1}}{\partial\omega} = -\Sigma_\Delta^{-1}\frac{\partial\Sigma_\Delta}{\partial\omega}\Sigma_\Delta^{-1}
\tag{51}
$$

$$
\frac{\partial^2 \Sigma_\Delta^{-1}}{\partial\omega^2} = -\left(\frac{\partial\Sigma_\Delta^{-1}}{\partial\omega}\frac{\partial\Sigma_\Delta}{\partial\omega}\Sigma_\Delta^{-1} + \Sigma_\Delta^{-1}\frac{\partial^2 \Sigma_\Delta}{\partial\omega^2}\Sigma_\Delta^{-1} + \Sigma_\Delta^{-1}\frac{\partial\Sigma_\Delta}{\partial\omega}\frac{\partial\Sigma_\Delta^{-1}}{\partial\omega}\right)
\tag{52}
$$

$$
\frac{\partial^2 \ln|\Sigma_\Delta|}{\partial\omega^2} = \text{Tr}\left(\frac{\partial\Sigma_\Delta^{-1}}{\partial\omega}\frac{\partial\Sigma_\Delta}{\partial\omega} + \Sigma_\Delta^{-1}\frac{\partial^2 \Sigma_\Delta}{\partial\omega^2}\right)
\tag{53}
$$

in which $\mathrm{Tr}(*)$ stands for the trace of $*$ and

$$\frac{\partial \Sigma_\Delta}{\partial \omega} = 2J_\omega^T \omega J_\omega \tag{54}$$

$$\frac{\partial^2 \Sigma_\Delta}{\partial \omega^2} = 2J_\omega^T J_\omega \tag{55}$$

For the Gibson et al. (2016) dataset, the maximum likelihood estimate of the overdispersion parameter is 0.672 Ma with a standard error of 0.16 Ma.

6   Dealing with skewed error distributions

All the free parameters in the regression algorithm (t, α, β and ω) are strictly positive quantities. This positivity constraint manifests itself in skewed error distributions. For example, when the four parameter algorithm of Section 5 is applied to datasets that exhibit little or no overdispersion ($\omega \approx 0$), then the usual '2-sigma' error bounds can cross over into physically impossible negative data space. This section of the paper introduces two ways to deal with this problem.

A first solution is to obtain asymmetric uncertainty bounds for ω using a profile likelihood approach (Galbraith, 2005; Vermeesch, 2018). First, maximise Equation 30 for the four parameters t, α, β and ω. Denote the corresponding log-likelihood value by $\mathcal{L}_m$. Second, consider a range of values for ω around the maximum likelihood estimate. For each of these values, maximise $\mathcal{L}$ for t, α and β whilst keeping ω fixed. Denote the corresponding log-likelihood by $\mathcal{L}_\omega$. Finally, a 95% confidence region for ω is obtained by collecting all the values of ω for which $\mathcal{L}_\omega > \mathcal{L}_m - 3.85/2$, where 3.85 corresponds to the 95th percentile of a chi-square distribution with one degree of freedom.

Figure 2 illustrates the profile likelihood method using the Gibson et al. (2016) dataset. The same procedure can also be applied to t, α and β, in order to obtain asymmetric confidence intervals for those parameters if needed. This would be particularly useful for very young samples.

A second and more pragmatic approach to dealing with the positivity constraint is to simply redefine the regression parameters in terms of logarithmic quantities. This is done by replacing Equations 12, 13 and 43 with:

$$K = X - U \exp[\beta_*]W\gamma - \exp[\lambda_{35}e^{t_*}] + 1 \tag{56}$$

$$L = Y - \exp[\alpha_*]W\gamma - \exp[\lambda_{38}e^{t_*}] + 1 \tag{57}$$

$$\Sigma_\Delta = J\Sigma J^T + J_\omega \exp[\omega_*]^2 J_\omega^T \tag{58}$$

respectively, and maximising Equation 30 with respect to t_*, α_*, β_* and ω_*. The standard errors for these log parameters (again obtained from the Fisher Information matrix) can then be converted to asymmetric confidence intervals for t, α, β and ω. Applying this approach to the Gibson et al. (2016) dataset yields results that are similar to those obtained using the profile
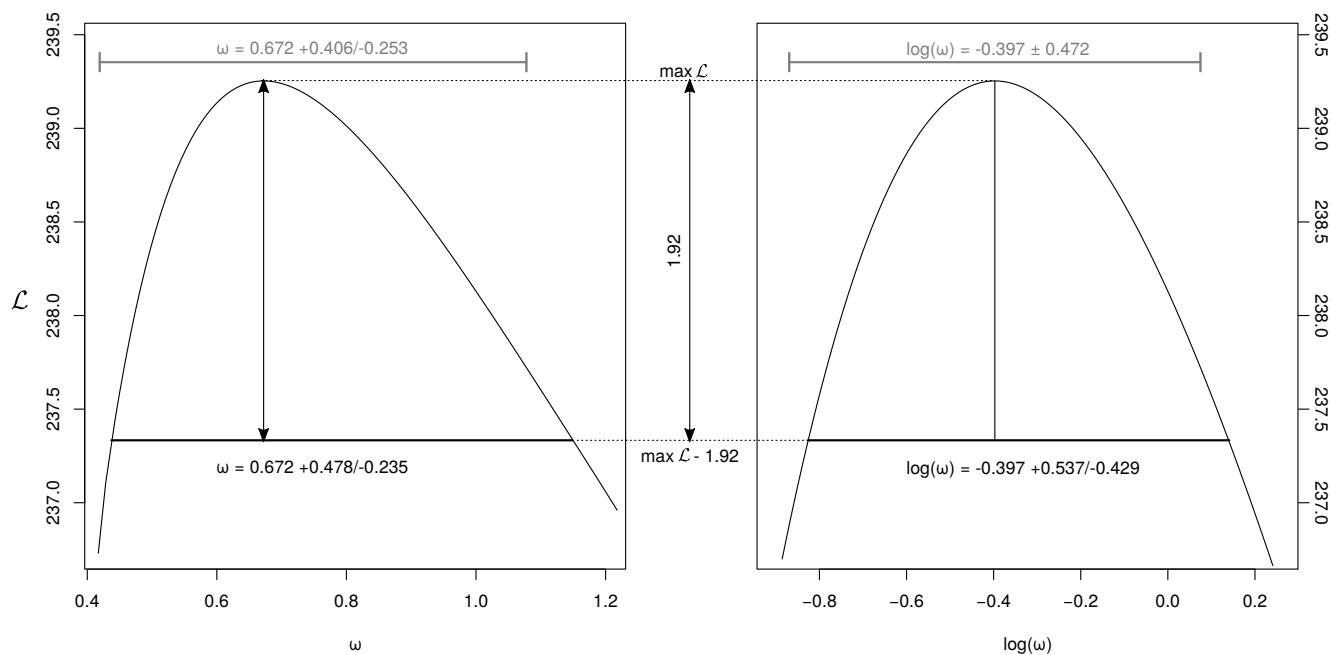
Figure 2. Profile log-likelihood intervals of the overdispersion parameter ω (black, left) and $\log(\omega)$ (black, right) for the Gibson et al. (2016) dataset. The set of ω-values whose log-likelihood fall within a range of 1.92 from the maximum value define an asymmetric 95% confidence interval. Alternatively, a standard symmetric confidence interval for $\log(\omega)$ (grey, right) can be mapped to an asymmetric confidence interval for ω (grey, left). The two approaches yield similar results.

235   log-likelihood method (Figure 2). Besides generating realistic confidence regions, the logarithmic reparameterisation of the likelihood function has the added benefit increasing the numerical stability of the maximum likelihood method.

7   Detrital samples

So far we have assumed that all the U-Th-Pb measurements are cogenetic and share the same common Pb composition. This assumption is generally not valid for detrital minerals, which tend to contain a mixture of provenance components. In this case 240   the different crystals in a sample are not expected to plot along a single isochron line. However it is still possible to remove the common Pb component by making certain assumptions about the common Pb composition. One way to do this is to assume that the mineral of interest was extracted from a reservoir of known U-Th-Pb composition.

For example, using the two-stage lead evolution model of Stacey and Kramers (1975), it is possible to predict the [206]Pb/[208]Pb 245   and [207]Pb/[208]Pb ratios of the reservoir for any given time t. In other words, any given value of the concordia intersection age

determines parameters α and β of Equation 10. If $t < 3.7$ Ga, then

$$\alpha(t) = \frac{\left[\frac{206Pb}{204Pb}\right]_{3.7} + \left[\frac{238U}{204Pb}\right]_{sk}\left(e^{\lambda_{38}3.7} - e^{\lambda_{38}t}\right)}{\left[\frac{208Pb}{204Pb}\right]_{3.7} + \left[\frac{232Th}{204Pb}\right]_{sk}\left(e^{\lambda_{32}3.7} - e^{\lambda_{32}t}\right)} \tag{59}$$

$$\beta(t) = \frac{\left[\frac{207Pb}{204Pb}\right]_{3.7} + \frac{1}{U}\left[\frac{238U}{204Pb}\right]_{sk}\left(e^{\lambda_{35}3.7} - e^{\lambda_{35}t}\right)}{\left[\frac{208Pb}{204Pb}\right]_{3.7} + \left[\frac{232Th}{204Pb}\right]_{sk}\left(e^{\lambda_{32}3.7} - e^{\lambda_{32}t}\right)} \tag{60}$$

where $\left[^{206}Pb/^{204}Pb\right]_{3.7} = 11.152$, $\left[^{208}Pb/^{204}Pb\right]_{3.7} = 31.23$, $\left[^{207}Pb/^{204}Pb\right]_{3.7} = 12.998$, $\left[^{238}U/^{204}Pb\right]_{sk} = 9.74$, and $\left[^{232}Th/^{204}Pb\right]_{sk}$

36.84. Substituting $\alpha(t)$ and $\beta(t)$ for α and β in Equations 12–14 reduces the number of free parameters from three (α, β and t) to one (t). This provides a quick and numerically robust mechanism for common-Pb correction of detrital minerals.

8 Implementation in `IsoplotR`

The algorithms presented in this paper have been implemented in the `IsoplotR` software toolbox for geochronology (Vermeesch, 2018). The easiest way to use the U-Th-Pb isochron functions is via an online graphical user interface at `http://isoplotr.lo` Alternatively, the same functions can also be accessed from the command line, using the `R` programming language. This section of the paper presents some code snippets to illustrate the key functions involved. This brief tutorial assumes that the reader has `R` and `IsoplotR` installed on her/his computer. Further details about this are provided by Vermeesch (2018), and on the aforementioned website. First, we need to load `IsoplotR` into `R`:

```
library(IsoplotR)
```

Two new data formats have been added to `IsoplotR`'s existing six U-Pb formats, to accommodate datasets comprising ^{232}Th and ^{208}Pb. The Gibson et al. (2016) dataset has been included in the `IsoplotR` package as two data files (`UPb7.csv` and `UPb8.csv`), which are also available in the supplementary information of this paper.

`UPb7.csv` specifies the U-Th-Pb composition using the 'Wetherill' ratios ^{207}Pb/^{235}U, ^{206}Pb/^{238}U, ^{208}Pb/^{232}Th and ^{232}Th/^{238}U, whereas `UPb8.csv` uses the 'Tera-Wasserburg' ratios ^{238}U/^{206}Pb, ^{207}Pb/^{206}Pb, ^{208}Pb/^{206}Pb and ^{232}Th/^{238}U. Both data formats require that the analytical uncertainties and error correlations of all the ratios are specified. The following commands load the contents of `UPb7.csv` into a variable called `UPb`, and plot the data on a ^{208}Pb/^{232}Th vs. ^{206}Pb/^{238}U-concordia diagram:

```
UPb <- read.data('UPb7.csv',
                 method='U-Pb',format=7)
concordia(UPb,type=3)
```

Performing a discordia regression and visualising the results as a ^{208}Pb$_c$/^{206}Pb vs. ^{238}U/^{206}Pb isochron:

```
isochron(UPb,type=1)
```

which performs a three parameter regression without overdispersion. Accounting for overdispersion is done using the optional `model` argument:

```
275  fit <- isochron(UPb,type=1,model=3)
```

where `fit` is a variable that stores the numerical results of the isochron regression. This is a list of items that can be inspected by typing `fit` at the `R` command prompt. For example, the maximum likelihood estimates for t, α, β and ω are stored in `fit$par` and the covariance matrix in `fit$cov`. Changing `type` to `2` plots the regression results as a $^{208}Pb_c/^{207}Pb$ vs. $^{235}U/^{207}Pb$ isochron. The isochron results can also be visualised on the concordia diagram:

```
280  concordia(UPb,type=2,show.age=2)
```

where `type=2` produces a Tera-Wasserburg diagram and the `show.age` argument adds a three-parameter regression line to it. Change this to `show.age=4` for a four-parameter fit.

9   Discussion and future developments

This paper introduced a new algorithm for common Pb correction by joint regression of all Pb isotopes of U and Th. The algorithm was successfully applied to a monazite dataset by Gibson et al. (2016). With a Th/U-ratio of ~ 10, the Gibson et al. (2016) sample represents a 'worst case scenario', because the presence of significant amounts of radiogenic ^{208}Pb complicates the ^{208}Pb-based common Pb correction. The fact that the Gibson et al. (2016) test case is successful holds great promise for the application of the new algorithm to Th-poor materials such as carbonates.

The ingrowth of radiogenic Pb described by Equations 2–4 assumes initial secular equilibrium between all the intermediate daughters in the U-Th-Pb decay chains. The new discordia regression algorithm can be modified to accommodate departures from this assumption. In fact, such disequilibrium corrections have already been implemented in `IsoplotR`, using the matrix derivative approach of McLean et al. (2016). A manuscript detailing these calculation is in preparation by the latter author. The disequilibrium correction is particularly useful for applications to young carbonates, whose initial $^{234}U/^{238}U$ and $^{230}Th/^{238}U$ activity ratios may be far out of equilibrium.

The new discordia regression algorithm is based on the method of maximum likelihood, and accounts for correlated uncertainties between variables. For example, the analytical uncertainties of the $^{208}Pb/^{232}Th$ and $^{232}Th/^{238}U$ ratios in the Gibson et al. (2016) dataset are characterised by correlation coefficients of ca. -0.6. However geochronological datasets are often associated with equally significant error correlations *between samples* (Vermeesch, 2015). The algorithm presented in this paper easily handles such correlations, which carry *systematic uncertainty*. It suffices to replace the zero values in the upper left $[3n \times 3n]$ sub-matrix of Equation 19 with non-zero values. Unfortunately, there currently exist no algorithms that keep track of inter-sample error correlations in the context of U-Pb geochronology. Doing so will require a new generation of low level data processing software.

This new generation software will also need to deal with a second issue that negatively affects the accuracy of the U(-Th)-Pb method, which is apparent from Figures 1.b and 1.c. After removing the radiogenic ^{208}Pb-component from the Gibson et al. (2016) dataset, the 95% confidence ellipse of one of the aliquots crosses over into negative ^{208}Pb$_c$/^{206}Pb and ^{208}Pb$_c$/^{207}Pb ratios. This nonsensical result is related to the issues discussed in Section 6. Isotopic data are strictly positive quantities that exhibit
310   skewed error distributions. 'Normal' statistical operations such as averaging and the calculation of '2-sigma' confidence intervals can produce counter-intuitive results when applied to such data.

In Section 6, the skewness of the fit parameters was removed by reformulating the regression algorithm in terms of logarithmic quantities. Similarly, Vermeesch (2015) showed that the skewness of isotopic compositions can be removed using
315   log-ratios, in the context of ^{40}Ar/^{39}Ar geochronology. McLean et al. (2016) introduced the same approach to in-situ U-Pb geochronology by LA-ICP-MS. Future software development will allow analysts to export their U-Th-Pb isotopic data directly as logratios and covariance matrices. Such a data structure can still be analysed with the new discordia regression algorithm, after a logarithmic change a variables for X, Y, Z and W in Equations 12, 13 and 14.

320   The U-Pb method is one of the most powerful and versatile methods in the geochronological toolbox. With two isotopes of the same parent (^{235}U and ^{238}U) decaying to two different isotopes of the same daughter (^{207}Pb and ^{206}Pb), the U-Pb method offers an internal quality control that is absent from most other geochronological techniques. U-bearing minerals often contain significant amounts of Th, which decays to ^{208}Pb. However until this day geochronologists have not frequently used this additional parent-daughter pair to its full potential. It is hoped that the algorithm and software presented in this paper will
325   change this situation.

Data availability. Datasets `UPb7.csv` and `UPb8.csv` are included in the supplementary information.

Author contributions. As the sole author of this paper, PV did all the work and wrote the entire paper.

Competing interests. PV does not have any competing interests.

Acknowledgements. PV would like to thank Randy Parrish, Phil Hopley and John Cottle for stimulating discussions that prompted the writing
330   of this paper.

References

Galbraith, R. F.: Statistics for fission track analysis, CRC Press, 2005.

Gibson, R., Godin, L., Kellett, D. A., Cottle, J. M., and Archibald, D.: Diachronous deformation along the base of the Himalayan metamorphic core, west-central Nepal, Geological Society of America Bulletin, 128, 860–878, 2016.

335   Hiess, J., Condon, D. J., McLean, N., and Noble, S. R.: ^{238}U/^{235}U systematics in terrestrial uranium-bearing minerals, Science, 335, 1610–1614, 2012.

Ludwig, K. R.: On the treatment of concordant uranium-lead ages, Geochimica et Cosmochimica Acta, 62, 665–676, https://doi.org/10.1016/S0016-7037(98)00059-3, 1998.

McLean, N. M., Bowring, J. F., and Gehrels, G.: Algorithms and software for U-Pb geochronology by LA-ICPMS, Geochemistry, Geo-
340   physics, Geosystems, 17, 2480–2496, 2016.

McLean, N. M., Smith, C. J. M., Roberts, N. M. W., and Richards, D. A.: Connecting the U-Th and U-Pb Chronometers: New Algorithms and Applications, AGU Fall Meeting Abstracts, 2016.

Stacey, J. and Kramers, J.: Approximation of terrestrial lead isotope evolution by a two-stage model, Earth and Planetary Science Letters, 26, 207–221, 1975.

345   Vermeesch, P.: Revised error propagation of ^{40}Ar/^{39}Ar data, including covariances, Geochimica et Cosmochimica Acta, 171, 325–337, 2015.

Vermeesch, P.: IsoplotR: a free and open toolbox for geochronology, Geoscience Frontiers, 9, 1479–1493, 2018.